

Stellar mass Primordial Black Holes as Cold Dark Matter

J. L. G. Sobrinho^{1,2*}, P. Augusto^{3†}

¹*Faculdade de Ciências Exatas e da Engenharia, Universidade da Madeira, Campus da Penteada, 9020-105 Funchal, Portugal*

²*Instituto de Astrofísica e Ciências do Espaço, Universidade de Lisboa, OAL, Tapada da Ajuda, 1349-018 Lisboa, Portugal*

³*Faculdade de Medicina da Universidade do Porto, Al. Prof. Hernâni Monteiro, 4200-319, Porto, Portugal*

Accepted 2020 May 19. Received 2020 May 13; in original form 2020 March 12

ABSTRACT

Primordial Black Holes (PBHs) might have formed in the early Universe due to the collapse of density fluctuations. PBHs may act as the sources for some of the gravitational waves recently observed. We explored the formation scenarios of PBHs of stellar mass, taking into account the possible influence of the QCD phase transition, for which we considered three different models: Crossover Model (CM), Bag Model (BM), and Lattice Fit Model (LFM). For the fluctuations, we considered a running-tilt power-law spectrum; when these cross the $\sim 10^{-9}$ – 10^{-1} s Universe horizon they originate 0.05 – $500 M_{\odot}$ PBHs which could: i) provide a population of stellar mass PBHs similar to the ones present on the binaries associated with all known gravitational wave sources; ii) constitute a broad mass spectrum accounting for $\sim 76\%$ of all Cold Dark Matter (CDM) in the Universe.

Key words: black hole physics - gravitational waves - cosmology: early Universe - cosmology: dark matter

1 INTRODUCTION

The Laser Interferometer Gravitational-Wave Observatory (LIGO) identified gravitational waves emitted from the coalescence of a few binary black holes (BHs) located at distances of $\sim 10^2$ – 10^3 Mpc (Abbott et al. 2016a, 2017, 2019). The masses of these BHs are within the range 18 – $85 M_{\odot}$, suggesting the existence of an important population of binary BHs within that mass range (Abbott et al. 2016b). However, those masses are larger than those of typical binary BHs formed in astrophysical scenarios at the final stage of stellar evolution of main sequence stars (e.g. Blinnikov et al. 2016; Kohri & Terada 2018; Sasaki, et al. 2018; Scelfo, et al. 2018; Belotsky et al. 2019).

Considering that Primordial Black Holes (PBHs) might have formed in the early Universe as a consequence of the collapse of density fluctuations (Sobrinho, Augusto, & Gonçalves 2016, and references therein) it is plausible to consider that, at least, a fraction of these BH binaries could be of primordial origin (e.g. Bird et al. 2016; Clesse & García-Bellido 2017; Belotsky et al. 2019; Gow, et al. 2020).

Stellar mass PBHs with less than $60 M_{\odot}$ have been ruled out as the prime constituent of Cold Dark Matter (CDM) under the assumption of a monochromatic mass spectrum

(i.e. all stellar mass PBHs formed at a particular epoch, thus sharing a common mass, e.g. Dalcanton, et al. 1994). However, if a broad mass spectrum is allowed, then stellar mass PBHs might provide a relevant contribution to the Universe CDM (cf. Carr, Kühnel & Sandstad 2016).

During the radiation-dominated epoch of the Universe ($\sim 10^{-33}$ s to $\approx 2.37 \times 10^{12}$ s), fluctuations of quantum origin (that were stretched to scales much larger than the cosmological horizon during inflation) can re-enter the cosmological horizon giving rise to the formation of PBHs (García-Bellido, Linde & Wands 1996), provided that their amplitude (δ) is larger than a specific threshold value $\delta_c \simeq 0.43$ – 0.47 . However, during the QCD phase transition the value of δ_c decreases, favouring an even larger rate of PBH production (Sobrinho, et al. 2016, and references therein), in particular $\sim 0.5 M_{\odot}$ PBHs (e.g. Byrnes et al. 2018; Carr, Clesse & García-Bellido 2019a; Carr, et al. 2019b).

For a given scale k , the horizon crossing time (t_k) is given by (e.g. Blais et al. 2003)

$$ck = a(t_k)H(t_k) \quad (1)$$

where $a(t_k)$ is the scale factor and $H(t_k)$ the Hubble parameter.

The probability that a fluctuation crossing the horizon at some instant t_k has of collapsing and forming a PBH can be written as (e.g. Green 2015)

* E-mail: sobrinho@uma.pt

† E-mail: sciman@med.up.pt

$$\beta(t_k) = \frac{1}{\sqrt{2\pi}\sigma(t_k)} \int_{\delta_c}^{\infty} \exp\left(-\frac{\delta^2}{2\sigma^2(t_k)}\right) d\delta \quad (2)$$

where $\sigma(t_k)$ is the mass variance at the horizon crossing time which can be written as (e.g. Sobrinho 2011)

$$\sigma^2(k) = \int_0^{\frac{k_e}{k}} x^3 \delta_H^2(k_c) \frac{P(kx)}{P(k_c)} W_{TH}^2(x) W_{TH}^2\left(\frac{x}{\sqrt{3}}\right) dx \quad (3)$$

where k_e is the smallest scale generated by inflation, k_c some suitable pivot scale, $\delta_H^2(k_c)$ the amplitude of the density perturbation spectrum at k_c , W_{TH} represents the Fourier transform of the top-hat window function, and P the power spectrum of the density fluctuations which, for a running-tilt power-law spectrum (simplest version), is written as (e.g. Erfani 2014)

$$P(k) = P(k_c) \left(\frac{k}{k_c}\right)^{n(k)-1} \quad (4)$$

with $n(k)$, which specifies the dependence of the power spectrum on the comoving wavenumber k , the spectral index of the density perturbation (e.g. Carr, Gilbert, & Lidsey 1994; Bridle et al. 2003). The spectral index at the pivot scale is $n(k_c) = n_0 < 1$ (e.g. Erfani 2014).

In order for a non-negligible amount of PBHs to be produced, we must have a *blue spectrum*, i.e., we must have $n(k) > 1$ during some epochs (e.g. Blais et al. 2003), which is consistent with the CMB anisotropy (e.g. Erfani 2014; Carr, et al. 2016) and, so, we write

$$n(k) = n_0 + \sum_{i \geq 1} \frac{n_i}{(i+1)!} \left(\ln \frac{k}{k_c}\right)^i \quad (5)$$

with the parameters n_1 and n_2 the running of the spectral index and the running of the running of the spectral index (e.g. Erfani 2014), respectively.

Assuming that the majority of PBHs forming at a particular epoch have masses within the order of the horizon mass at that epoch, then stellar mass PBHs formed when the Universe was $\sim 10^{-5}$ – 10^{-3} s old, smack on the QCD epoch ($\sim 10^{-4}$ s) where we must study the threshold δ_c in order to learn about the stellar mass PBH formation. We do so in this paper, following our previous work (Sobrinho, et al. 2016), by using three different models for the QCD: Crossover Model (CM), Bag Model (BM), and Lattice Fit Model (LFM).

The aim of this paper, then, is to study the mass spectrum of PBHs within the extended stellar mass range 0.05–500 M_{\odot} , which covers all stellar mass PBHs. The paper is organized as follows: after reviewing, in Section 2, some key aspects concerning the cosmological density parameter of stellar mass PBHs, in Section 3 we introduce our approach to the spectral index $n(k)$. In Section 4 we present our results on the mass spectrum of stellar mass PBHs and, in Section 5, we conclude with a discussion on these results. Table 1 sums up key parameters that we use throughout this paper.

2 THE COSMOLOGICAL DENSITY OF PBH

The PBH density parameter for PBHs formed at a given instant $t = t_k$ can be written as (e.g. Niemeyer & Jedamzik 1998)

$$\Omega_{PBH}(t_k) = \frac{1}{M_H(t_k)} \int_{\delta_c}^{\infty} M_{PBH}(\delta, t_k) P(\delta, t_k) d\delta \quad (6)$$

with M_H the horizon mass at epoch t_k and M_{PBH} the PBH mass. Since (e.g. Niemeyer & Jedamzik 1998)

$$P(\delta, t_k) = \frac{1}{\sqrt{2\pi}\sigma(t_k)} \exp\left(-\frac{\delta^2}{2\sigma^2(t_k)}\right), \quad (7)$$

assuming only horizon-mass PBHs produced at each epoch ($M_{PBH}(\delta, t_k) = M_H(t_k)$) we get, from equations (2) and (6)

$$\Omega_{PBH}(t_k) = \beta(t_k). \quad (8)$$

Taking into account only non-evaporated PBHs formed at t_k , we get (e.g. Ricotti, Ostriker, & Mack 2008)

$$\Omega_{PBH}(t_k) [1 + z(t_k)] = \Omega_{PBH}(t_0, t_k) [1 + z(t_{eq})], \quad (9)$$

where z is the redshift, t_0 the current epoch, and $t_{eq} \approx 2.37 \times 10^{12}$ s the age of the Universe at the matter-radiation equality (cf. Sobrinho et al. 2016). From equation (8) and the definition of scale factor we get

$$\Omega_{PBH}(t_0, t_k) = \beta(t_k) \frac{1 + z(t_k)}{1 + z(t_{eq})} = \beta(t_k) \frac{a(t_{eq})}{a(t_k)}. \quad (10)$$

The present day number density of PBHs formed at a given epoch t_k can be written as (e.g. Sobrinho 2011)

$$n_{PBH}(t_0, t_k) = \rho_c(t_0) \frac{\Omega_{PBH}(t_0, t_k)}{M_H(t_k)} \quad (11)$$

where ρ_c is the critical density of the Universe. Integrating equation (10) we get the global value of Ω_{PBH} evaluated at the present day (i.e. the present day value of the PBH density parameter which takes into account all non-evaporated PBHs),

$$\Omega_{PBH}(t_0) = a(t_{eq}) \int_{t_*}^{t'} \frac{\beta(t_k)}{a(t_k)} dt_k, \quad (12)$$

where $t_* \sim 10^{-23}$ s (PBHs formed before t_* have already evaporated, e.g. Carr et al. 2010; Sobrinho & Augusto 2014) and $t' \sim 10^5$ s (PBHs formed at t' should have $\sim 10^{10} M_{\odot}$; BH candidates with masses above such value are not known, e.g. Saglia, et al. 2016). The current mass density of such PBHs, of course, must not exceed the total mass density of the Universe. By a similar integration of equation (11), the present day value of the PBH number density is given by

$$n_{PBH}(t_0) = \rho_c(t_0) \int_{t_*}^{t'} \frac{\Omega_{PBH}(t_0, t_k)}{M_H(t_k)} dt_k \quad (13)$$

or, if we are interested only on PBHs formed between two given instants t_1 and t_2 ($t_* \leq t_1 < t_2 \leq t'$)

$$n_{PBH}(t_0) = \rho_c(t_0) \int_{t_1}^{t_2} \frac{\Omega_{PBH}(t_0, t_k)}{M_H(t_k)} dt_k. \quad (14)$$

3 THE SPECTRAL INDEX OF THE DENSITY PERTURBATION

We consider a running-tilt power-law spectrum (equation 4) with a spectral index given by equation (5). The observational input needed to compute the spectral index are the parameters n_i measured at some pivot scale k_c . For $i \geq 3$ the values are still unknown, while the three known values

Table 1. Parameters used in this paper. References for the last column: [1] Erfani (2014); [2] Tanabashi, et al. (2018); [3] Planck Collaboration, et al. (2016).

Parameter	Description	Value	Reference
n_0	spectral index at the pivot scale (k_c)	0.9476	[1]
n_1	running of the spectral index	0.001	[1]
n_2	running of the running of the spectral index	0.0226	[1]
k_c	pivot scale	0.05 Mpc ⁻¹	[2]
$\delta_H^2(k_c)$	amplitude of the density perturbation spectrum at the pivot scale (k_c)	2.2×10^{-9}	[3]
$\rho_c(t_0)$	critical density of the Universe at current epoch (t_0)	8.62×10^{-27} kgm ⁻³	[2]
Ω_{CDM}	Cold Dark Matter density parameter	0.258	[2]

are presented in Table 1. Then, assuming $n_i = 0, i \geq 5$ we write, from equation (5)

$$n(k) = n_0 + \frac{n_1}{2} \ln \frac{k}{k_c} + \frac{n_2}{6} \left(\ln \frac{k}{k_c} \right)^2 + \frac{n_3}{24} \left(\ln \frac{k}{k_c} \right)^3 + \frac{n_4}{120} \left(\ln \frac{k}{k_c} \right)^4. \quad (15)$$

Now, the idea is to look for sets of values for n_3 and n_4 leading to relevant scenarios in terms of stellar mass PBH production, namely by seeking cases in which $n(k)$ exhibits a maximum, with $n_{max} > 1$, at some point $k = k_{max} > k_c$.

Equation (1) relates a given scale k with the instant t_k and, so, we here refer to k_{max} or to $t_{k_{max}}$ with the same meaning. Using $X = \ln(k_{max}/k_c)$ we write, following equation (15),

$$n_{max} = n_0 + \frac{n_1}{2}X + \frac{n_2}{6}X^2 + \frac{n_3}{24}X^3 + \frac{n_4}{120}X^4 \quad (16)$$

and, by definition,

$$\frac{dn}{dX}(k_{max}) = \frac{n_1}{2} + \frac{n_2}{3}X + \frac{n_3}{8}X^2 + \frac{n_4}{30}X^3 = 0. \quad (17)$$

Solving equations (16) and (17) we get

$$n_3 = -\frac{4(24n_0 - 24n_{max} + 9n_1X + 2n_2X^2)}{X^3} \quad \text{and} \quad (18)$$

$$n_4 = \frac{20(18n_0 - 18n_{max} + 6n_1X + n_2X^2)}{X^4}, \quad (19)$$

which allows us to relate (n_3, n_4) with the more meaningful quantities $(n_{max}, t_{k_{max}})$. Hence, for a given pair of values $(n_{max}, t_{k_{max}})$ we can determine, with the help of equations (18) and (19), and the n_0, n_1, n_2 values of Table 1, the corresponding values of n_3 and n_4 and, consequently, the curve for the spectral index $n(k)$ as given by equation (15). An example in a particular case showing a blue spectrum is presented in Figure 1.

4 THE MASS SPECTRUM OF STELLAR MASS PBH

We first determine the fraction of the Universe going into stellar mass PBHs at a given epoch t_k (cf. equation 2) us-

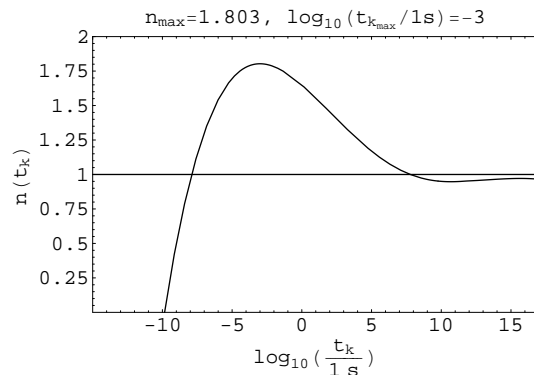


Figure 1. An example of the behaviour of $n(t_k)$ (equation 15) when $n_{max} = 1.803$ and $t_{k_{max}} = 10^{-3}$ s (the coordinates at the curve maximum). In this case we have a blue spectrum which is a requirement for PBH formation. From equations (18) and (19) we derive $n_3 = 0.0099$ and $n_4 = -0.0033$.

ing the three different models of Sobrinho, et al. (2016): i) Crossover Model (CM); ii) Bag Model (BM); iii) Lattice Fit Model (LFM).

4.1 Crossover Model (CM)

Equation (2) must now be written as

$$\beta_{CM}(t_k) = \frac{1}{\sqrt{2\pi}\sigma(t_k)} \int_{\delta_{c1}}^{\delta_c} \exp\left(-\frac{\delta^2}{2\sigma^2(t_k)}\right) d\delta + \beta_R(t_k) \quad (20)$$

where $\beta_R(t_k)$ is $\beta(t_k)$ (equation 2), now seen as the *contribution from radiation* (since the first term represents the contribution from the CM), while $\delta_{c1} < \delta_c$ is the threshold for PBH formation, valid during the QCD phase transition in the case of a CM (cf. Sobrinho et al. 2016). For epochs sufficiently away from the transition, $\delta_{c1} \approx \delta_c$ and equation (2) remains valid.

4.2 Bag Model (BM)

Now equation (2) is valid only up to some instant after which there is an additional window $[\delta_{c1}, \delta_{c2}] < \delta_c$ allowing PBH formation (Sobrinho et al. 2016), written as

$$\beta_{BM}(t_k) = \frac{1}{\sqrt{2\pi}\sigma(t_k)} \int_{\delta_{c1}}^{\delta_{c2}} \exp\left(-\frac{\delta^2}{2\sigma^2(t_k)}\right) d\delta + \beta_R(t_k). \quad (21)$$

Eventually, δ_{c2} reaches δ_c and we recover equation (20).

4.3 Lattice Fit Model (LFM)

We now consider yet another window $[\delta_{cA}, \delta_c]$ allowing PBH formation (cf. Sobrinho et al. 2016), writing equation (2) as

$$\beta_{LFM1}(t_k) = \frac{1}{\sqrt{2\pi}\sigma(t_k)} \int_{\delta_{cA}}^{\delta_c} \exp\left(-\frac{\delta^2}{2\sigma^2(t_k)}\right) d\delta + \beta_R(t_k). \quad (22)$$

Over a brief interval we might also have to consider the window $[\delta_{c1}, \delta_{c2}] < \delta_{cA}$ where

$$\beta_{LFM2}(t_k) = \frac{1}{\sqrt{2\pi}\sigma(t_k)} \int_{\delta_{c1}}^{\delta_{c2}} \exp\left(-\frac{\delta^2}{2\sigma^2(t_k)}\right) d\delta + \frac{1}{\sqrt{2\pi}\sigma(t_k)} \int_{\delta_{cA}}^{\delta_c} \exp\left(-\frac{\delta^2}{2\sigma^2(t_k)}\right) d\delta + \beta_R(t_k). \quad (23)$$

Again, at some point δ_{c2} reaches δ_{cA} and we return to equation (20).

4.4 Stellar mass PBHs formation (three models)

Following equation (15) (cf. Figure 1), by fixing $t_{k_{max}}$ we determine the allowed range of values for n_{max} , i.e., the range of values of n_{max} for which $\beta(t_k)$ does not exceed the observational constraints, which will depend on the model adopted for the QCD (equations 20–23). Within the stellar mass range 0.05–500 M_\odot these observational constraints are mainly obtained from gravitational lensing surveys, data from gravitational waves due to binary coalescences, and CMB anisotropies measured by Planck, with the maximum value allowed for $\beta(t_k)$ on the range $[10^{-11}, 10^{-8}]$ (for more details see Carr, et al. 2020).

We found, numerically (with Wolfram Mathematica 2005), that in order to fully cover the extended stellar mass range 0.05–500 M_\odot we should consider $1.4 \leq n_{max} \leq 2.0$ and $10^{-9} \text{ s} \leq t_{k_{max}} \leq 1 \text{ s}$. In Figure 2 we thus show the region on the $(n_{max}, \log(t_{k_{max}}/1 \text{ s}))$ plane where stellar mass PBH formation is possible, between: i) the ‘forbidden region’ where the amount of formed stellar mass PBH would violate the observational constraints; ii) ‘No PBH formation’, actually meaning that this is negligible (less than one stellar mass PBH within the entire observable Universe – see Section 4.5).

For a given value of $t_{k_{max}}$ the fraction of the Universe going into PBHs, $\beta(t_k)$, will be maximum if the corresponding value of n_{max} is the one located over the solid curve in Figure 2. Results for a selection of cases in such conditions are given in Figure 3 and Table 2.

As seen in Sections 4.1–4.3, for epochs sufficiently away from the influence of the QCD, the dominant term in equations (20) to (23) is $\beta_R(t_k)$, and a *radiation peak* is seen around $t_{k_{max}}$ (e.g. Figure 3e). On the other hand, at epochs close to the QCD epoch, a *QCD peak* shows up, with the $t_{k_{max}}$ location dependent on the model (e.g. Figure 3b).

When $t_{k_{max}} = 10^{-9} \text{ s}$ we may consider $n_{max} = 1.523$ for all the three QCD models in order to maximize the number of PBHs without violating the observational constraints

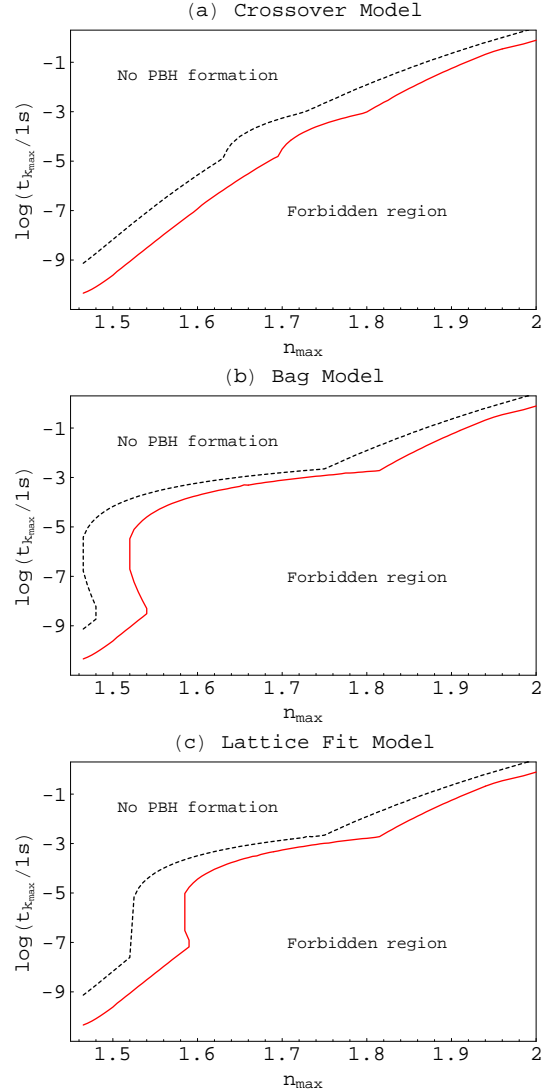


Figure 2. The curve in the $(n_{max}, \log(t_{k_{max}}/1 \text{ s}))$ plane indicating which parameter values lead to stellar mass PBH formation, according to each of the three QCD models (CM, BM, LFM). Below the solid curve, PBH formation is not allowed since it would violate the observational constraints (Carr, et al. 2020). Above the dashed line, PBH formation is allowed although in negligible numbers (less than one PBH within the observable Universe). The region of interest, as regards PBH formation, is the one located between the two lines, with the most favourable situations on the solid curve: the number density of PBHs decreases as one moves from the solid line towards the dashed line.

(Table 2). The $\beta(t_k)$ curve for this case is shown in Figure 3a. Notice that for both the CM and LFM we have the same $\beta(t_k)$ curve (left portion of the curve in Figure 3a, which corresponds to a radiation peak). This happens because we are considering fluctuations that crossed the horizon sufficiently before the QCD epoch. If we consider a BM instead, then we cannot neglect the contribution from the QCD (cf. equation 21) and as a result we have, in addition, a QCD peak (although not quite as high as the radiation peak).

In Figure 3b we show the curve for $\beta(t_k)$ when $t_{k_{max}} = 10^{-7} \text{ s}$ and with n_{max} assuming the values 1.599 (CM), 1.524 (BM), and 1.593 (LFM) – Table 2. Notice that

we are considering, for each QCD model, different values of n_{max} in order to reach the maximum production of PBHs allowed for each case at the considered epoch. Although the CM curve still consists entirely of a radiation peak, now the BM curve is fully dominated by the QCD peak. As for the LFM curve we have the presence of the two peaks (namely, a radiation peak on the left and a QCD peak on the right).

Moving to Figure 3c we show the curves for $\beta(t_k)$ when $t_{k_{max}} = 10^{-5}$ s with n_{max} assuming the values 1.686 (CM), 1.530 (BM), and 1.587 (LFM) – Table 2. In terms of the CM we now get a radiation peak as well as a QCD peak, the latter just emerging on the right side of the curve, while the BM and LFM curves are completely dominated by their sharp QCD peaks.

In the case $t_{k_{max}} = 10^{-3}$ s (Figure 3d) n_{max} assumes the values 1.803 (CM), 1.732 (BM), and 1.752 (LFM) – Table 2. In the case of a CM (see also Figure 1) we get a radiation peak and a QCD peak which join (the latter more on the left), forming some sort of plateau in the $\beta(t_k)$ curve. The BM and LFM are still dominated by the QCD peak, which now appears on the left, although the radiation peak is more obvious.

Finally, in Figure 3e we show the curve for $\beta(t_k)$ when $t_{k_{max}} = 10^{-1}$ s and $n_{max} = 1.920$. In this case we are dealing with fluctuations that crossed the horizon sufficiently after the QCD epoch and, so, all the three QCD models share the same curve (and, hence, the same value for n_{max} – Table 2) which is characterized by a radiation peak.

4.5 The mass spectrum of stellar mass PBHs

We can interpret the curve $n_{PBH}(t_0, t_k)$ (equation 11) as a mass spectrum: the *PBH mass spectrum*. For each of the cases shown in Figure 3 we divided the curve $n_{PBH}(t_0, t_k)$ into different portions, each corresponding to an order of magnitude, and integrated these in order to obtain the number density of PBHs of a given mass (equation 14). We have assumed, as a first approach, that PBHs formed at a particular epoch are uniformly distributed throughout the Universe.

The PBH mass spectrum of our best result is shown in Figure 4 ($t_{k_{max}} = 10^{-3}$ s, $n_{max} = 1.803$, QCD/CM – see also Figures 1 and 3d), arising as a consequence of the plateau formed by the proximity of the radiation and QCD peaks (cf. Figure 3d). From equation (12) we get, for this case, $\Omega_{PBH} \approx 0.197$. So, from Table 1, we get:

$$\frac{\Omega_{PBH}}{\Omega_{CDM}} = \frac{0.197}{0.258} = 0.763. \quad (24)$$

Thus, about 76% of all CDM might be constituted by PBHs, 44% in the form of $5 M_\odot$ and 32% in the form of $50 M_\odot$ ones. Our second best result gives a 12% contribution ($t_{k_{max}} = 10^{-5}$ s, $n_{max} = 1.686$, again QCD/CM – see Figure 3c). We have, thus, compiled all cases exemplified in this paper (Figures 2 and 3) in Table 3, focusing on results on the extended stellar mass range ($0.05\text{--}500 M_\odot$), which surely includes all stellar mass PBHs.

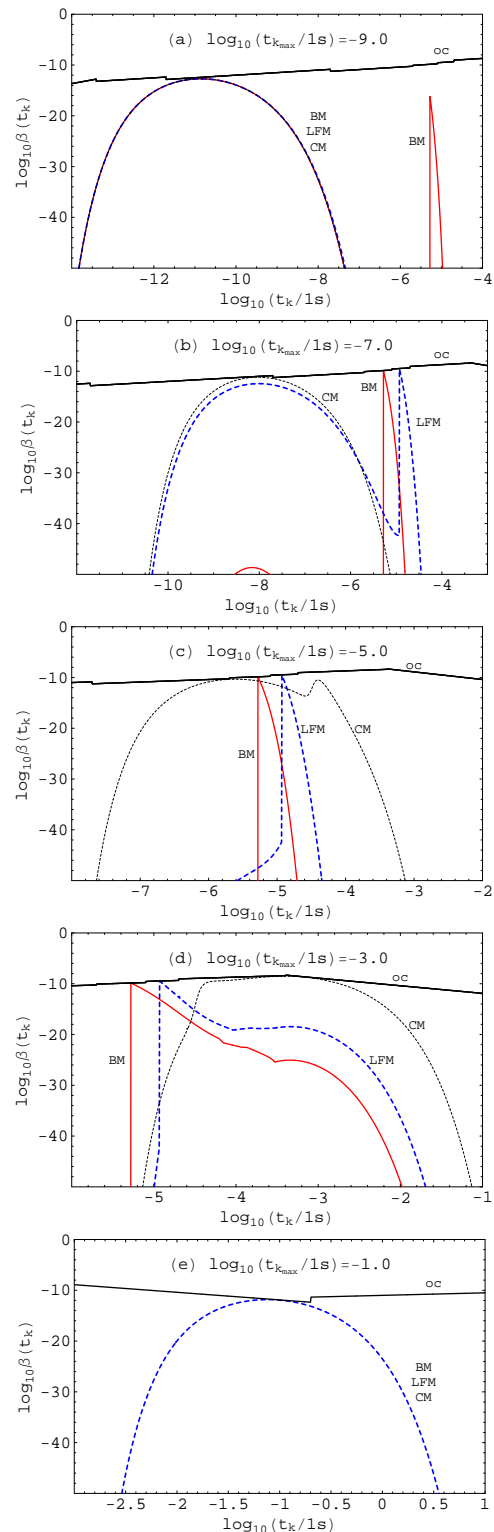


Figure 3. The fraction of the Universe going into stellar mass PBHs when: (a) $t_{k_{max}} = 10^{-9}$ s; (b) $t_{k_{max}} = 10^{-7}$ s; (c) $t_{k_{max}} = 10^{-5}$ s; (d) $t_{k_{max}} = 10^{-3}$ s, and (e) $t_{k_{max}} = 10^{-1}$ s. Each curve is labeled according to the corresponding QCD model (CM, dotted; BM, continuous; LFM, dashed). The curve labeled ‘oc’ in the top of each figure represents the observational constraints. In (e) a dominating ‘radiation peak’ is seen, centred near $t_{k_{max}}$ (for all models) while a secondary ‘QCD peak’ arises for cases like the ones seen in (b), with the centre-of-peak dependent on the model. Note that the situation exemplified in (d), for the CM, is the one of Figure 1.

Table 2. Results for a selection of studied cases which imply maximum stellar mass PBH formation (on the solid lines of Figure 2): **(1)** the instant when the fluctuation crosses the Universe horizon; **(2)** the maximum value attained by the spectral index (retrieved from Figure 2); **(3)** the corresponding QCD model (CM, BM or LFM); **(4)** parameter n_3 , from equation (18); **(5)** parameter n_4 , from equation (19); **(6)** related Figure(s). The highlighted example is the one presented in Figure 1.

(1)	(2)	(3)	(4)	(5)	(6)
$\log(t_{k_{max}}/1 \text{ s})$	n_{max}	QCD model	n_3	n_4	Fig.
-9	1.523	CM,BM,LFM	-0.0031	0.000078	3a
-7	1.599	CM	-0.0013	-0.00030	3b
-7	1.524	BM	-0.0021	-0.00014	3b
-7	1.593	LFM	-0.0014	-0.00029	3b
-5	1.686	CM	0.0023	-0.0012	3c
-5	1.530	BM	-0.00030	-0.00062	3c
-5	1.587	LFM	0.00064	-0.00082	3c
-3	1.803	CM	0.0099	-0.0033	1,3d
-3	1.732	BM	0.0081	-0.0028	3d
-3	1.752	LFM	0.0086	-0.0030	3d
-1	1.920	CM,BM,LFM	0.026	-0.0084	3e

Table 3. The PBH stellar mass spectrum (0.05–500 M_\odot) according to the three QCD models (CM: Crossover Model; BM: Bag Model; LFM: Lattice Fit Model) for the relevant examples of Figure 3 (between curved brackets, the $\log(t_{k_{max}}/1 \text{ s})$ is shown) that give results in that mass range in the most favourable situations (solid lines in Figure 2), from where the n_{max} values come from. The values shown in percentage between square brackets are the $> 10^{-5}$ % contribution to the fraction of CDM, in each case.

M_\odot	N/Mpc ³										
	10 ⁻⁷	0.1	1	10	100	10 ³	10 ⁴	10 ⁸	10 ⁹	10 ¹⁰	10 ¹¹
0.05					LFM(-7)		CM(-7)				CM(-5) [9%]
0.5						CM(-3)			BM(-7) [0.4%]	CM(-5) [3%]	
						BM(-9)			LFM(-7) [0.6%]	BM(-3) [2%]	
									BM(-5) [0.6%]	LFM(-3) [2%]	
									LFM(-5) [0.7%]		
5			BM(-3)			LFM(-3)		CM(-5) [0.3%]		CM(-3) [44%]	
50	BM(-3)	LFM(-3)							CM(-3) [32%]		
500				CM(-1)			CM(-3)				
				BM(-1)			[0.001%]				
				LFM(-1)							

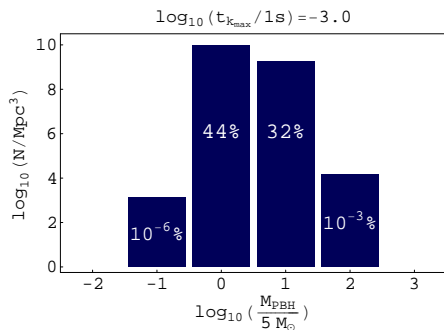


Figure 4. The PBH mass spectrum when $t_{k_{max}} = 10^{-3} \text{ s}$ and $n_{max} = 1.803$ (CM) – cf. Figures 1 and 3d. The values in percentage represent the contribution to the fraction of CDM in each case. See text and Table 3 for more details.

5 DISCUSSION

The sources of many of the recently detected gravitational waves by LIGO are likely BH binaries with masses within the range 18–85 M_\odot , suggesting an important population of binary BHs with stellar masses. However, it is not certain that these BHs result from the final stages of stellar evolution. Instead, it is quite plausible that these binaries are primordial in origin. So, this paper explored scenarios for the formation of stellar mass PBHs (0.05–500 M_\odot). Although PBHs have not yet been observed directly in the Universe (nevertheless, see, e.g., Sobrinho & Augusto 2014, for interesting possibilities) there are several observational constraints on the maximum number of PBHs of a given mass that could, eventually, have been formed at a given epoch.

PBHs can be formed from the collapse of overdense regions in the early Universe, provided that the amplitude of the density fluctuation is greater than some critical threshold δ_c . During the QCD phase transition (when

$M_H \sim 0.5 M_\odot$) the value of δ_c experiences a reduction which further favors PBH formation. We have, thus, studied three different models for the QCD phase transition (CM, BM, and LFM) using a running-tilt power-law spectrum for the primordial density fluctuations. We selected five representative cases ($t_{k_{max}} = 10^{-9}, 10^{-7}, 10^{-5}, 10^{-3}$, and 10^{-1} s), covering the full $0.05\text{--}500 M_\odot$ range (corresponding to the range $1.4 \leq n_{max} \leq 2.0$), with $t_{k_{max}}$ the instant when the fluctuation crosses the horizon and n_{max} the amplitude of the spectral index at that instant.

There are about 2×10^{12} galaxies in the Universe, with comoving densities of $0.1\text{--}1 \text{ Mpc}^{-3}$ and typical masses of $10^{10} M_\odot$ (Conselice et al. 2016). On a QCD/CM, in particular when $t_{k_{max}} = 10^{-3}$ s, we estimated $10^9\text{--}10^{10}$ PBH/Mpc³ (Table 3) with $5\text{--}50 M_\odot$. Therefore, from the comoving density of galaxies, one would expect $\sim 10^{9\text{--}11}$ PBHs per galaxy.

Although, at this stage, the actual model at the QCD epoch is not known, finding a monochromatic peak at $\sim 0.5 M_\odot$ will favour a BM or LFM model, while a broader mass spectrum ($5\text{--}50 M_\odot$) will suggest a CM. Thus, if the latter applies, PBHs are excellent candidates for the observed gravitational wave cases, since their numbers could be as high as 76% of the Universe CDM!

As regards future work we aim to consider the clustering of PBHs, in particular the formation of stellar mass PBH binaries that could account for the observed gravitational wave sources.

REFERENCES

- Abbott, B. P., et al., 2016a, PhRvL, 116, 061102
 Abbott B. P., et al., 2016b, ApJ, 818, L22
 Abbott B. P., et al., 2017, PhRvL, 118, 221101
 Abbott B. P., et al., 2019, PhRvX, 9, 031040
 Belotsky K. M., et al., 2019, EPJC, 79, 246
 Bird S., Cholis I., Muñoz J. B., Ali-Haïmoud Y., Kamionkowski M., Kovetz E. D., Raccanelli A., Riess A. G., 2016, PhRvL, 116, 201301
 Blais D., Bringmann T., Kiefer C., Polarski D., 2003, Phys. Rev. D, 67, 024024
 Bridle S. L., Lewis A. M., Weller J., Efstathiou G., 2003, MNRAS, 342, L72
 Blinnikov S., Dolgov A., Porayko N. K., Postnov K., 2016, JCAP, 2016, 036
 Byrnes C. T., Hindmarsh M., Young S., Hawkins M. R. S., 2018, JCAP, 2018, 041
 Carr B., Clesse S., García-Bellido J., 2019a, arXiv, arXiv:1904.02129
 Carr B., Clesse S., García-Bellido J., Kuhnel F., 2019b, arXiv, arXiv:1906.08217
 Carr B. J., Gilbert J. H., Lidsey J. E., 1994, PhRvD, 50, 4853
 Carr B. J., Kohri K., Sendouda Y., Yokoyama J., 2010, Phys. Rev. D, 81, 104019
 Carr B., Kohri K., Sendouda Y., Yokoyama J., 2020, arXiv, arXiv:2002.12778
 Carr B., Kühnel F., Sandstad M., 2016, PhRvD, 94, 83504
 Clesse S., García-Bellido J., 2017, PDU, 15, 142
 Conselice C. J., Wilkinson A., Duncan K., Mortlock A., 2016, ApJ, 830, 83
 Dalcanton J. J., Canizares C. R., Granados A., Steidel C. C., Stocke J. T., 1994, ApJ, 424, 550
 Erfani E., 2014, PhRvD, 89, 083511
 García-Bellido J., Linde A., Wands D., 1996, PhRvD, 54, 6040
 Gow A. D., Byrnes C. T., Hall A., Peacock J. A., 2020, JCAP, 2020, 031
 Green A. M., 2015, in Calmet X., ed., Quantum Aspects of Black Holes. Springer, London, p. 129
 Kohri K., Terada T., 2018, CQGrA, 35, 235017
 Niemeyer J. C., Jedamzik K., 1998, PhRvL, 80, 5481
 Planck Collaboration, et al., 2016, A&A, 594, A20
 Ricotti M., Ostriker J. P., Mack K. J., 2008, ApJ, 680, 829
 Saglia R. P., et al., 2016, ApJ, 818, 47
 Sasaki M., Suyama T., Tanaka T., Yokoyama S., 2018, CQGrA, 35, 063001
 Scelfo G., Bellomo N., Raccanelli A., Matarrese S., Verde L., 2018, JCAP, 2018, 039
 Sobrinho J. L. G., 2011, PhD thesis, Univ. da Madeira available at: <http://digituma.uma.pt/handle/10400.13/235>
 Sobrinho J. L. G., Augusto P., 2014, MNRAS, 441, 2878
 Sobrinho J. L. G., Augusto P., Gonçalves A. L., 2016, MNRAS, 463, 2348
 Tanabashi M., et al., 2018, PhRvD, 98, 30001
 Wolfram Research Inc., Mathematica, Version 5.0. Wolfram Research, Inc., Champaign, IL (2005)